NUCLEAR SCIENCE AND TECHNIQUES **26**, 040601 (2015)

Simulation of nucleate boiling under ANSYS-FLUENT code by using RPI model coupling with artificial neural networks*

Brahim Mohamedi,[1,2,†] Salah Hanini,[2] Abdelrahmane Ararem,[1] and Nacim Mellel[1]

[1]*Birine Nuclear Research Center B.P.180, Ain Oussera 17200, Algérie*
[2]*LBMPT Dr Yahia Farés University, Médéa 26000, Algérie*

(Received September 18, 2014; accepted in revised form November 3, 2014; published online August 20, 2015)

The present study is to develop a new user-defined function using artificial neural networks intent Computational Fluid Dynamics (CFD) simulation for the prediction of water-vapor multiphase flows through fuel assemblies of nuclear reactor. Indeed, the provision of accurate material data especially for water and steam over a wider range of temperatures and pressures is an essential requirement for conducting CFD simulations in nuclear engineering thermal hydraulics. Contrary to the commercial CFD solver ANSYS-CFX, where the industrial standard IAPWS-IF97 (International Association for the Properties of Water and Steam-Industrial Formulation 1997) is implemented in the ANSYS-CFX internal material database, the solver ANSYS-FLUENT provides only the possibility to use equation of state (EOS), like ideal gas law, Redlich-Kwong EOS and piecewise polynomial interpolations. For that purpose, new approach is used to implement the thermophysical properties of water and steam for subcooled water in CFD solver ANSYS-FLUENT. The technique is based on artificial neural networks of multi-layer type to accurately predict 10 thermodynamic and transport properties of the density, specific heat, dynamic viscosity, thermal conductivity and speed of sound on saturated liquid and saturated vapor. Temperature is used as single input parameter, the maximum absolute error predicted by the artificial neural networks ANNs, was around 3%. Thus, the numerical investigation under CFD solver ANSYS-FLUENT becomes competitive with other CFD codes of which ANSYS-CFX in this area. In fact, the coupling of the Rensselaer Polytechnical Institute (RPI) wall boiling model and the developed Neural-UDF (User Defined Function) was found to be useful in predicting the vapor volume fraction in subcooled boiling flow.

Keywords: User defined function (UDF), Computational fluid dynamics, IAPWS-IF97, ANSYS-FLUENT, Multilayer perceptron (MLP), Rensselaer polytechnical institute

DOI: 10.13538/j.1001-8042/nst.26.040601

I. INTRODUCTION

The present study is concerned with artificial neural networks support to the ongoing study on nucleate boiling. The focus is placed on numerical simulations of the preconditioning of two phase flows in a circular tube with heated wall under pressurized conditions. Computational fluid dynamic techniques show increasing promise for the simulation of subcooled nucleate boiling [1]. The commercial Computational Fluid Dynamics (CFD) solver ANSYS-FLUENT is employed as the computational platform and the Eulerian method in combination with RPI boiling model is used, where the phases are assumed to be interpenetrating continua. This model is the most general and complex of all multiphase flow models. The advantage of ANSYS-FLUENT is the number of turbulent model adapted to special case. On the other hand, CFX was the go-to code for turbomachinery.

Contributions are made towards an improved flow boiling model under Pressurized Water Reactor (PWR) conditions by carrying out detailed CFD analyses based on experimental data of void distributions in heated tubes. When a heated surface exceeds the saturation temperature of surrounding coolant, boiling on the surface becomes possible. Bubbles formed on the heated surface depart the surface and are transported by the bulk fluid, such that a condition of two-phase flow is said to exist. Depending on degree of subcooling and length of the heated tube, the bubbles may or may not condense and collapse prior to exiting the tube. In subcooled boiling this process results in further heating of the fluid toward the saturation temperature. In saturated or bulk boiling, bubbles can be transported along the entire length of the heated tube without collapsing [2].

In Rensselaer Polytechnical Institute (RPI) wall boiling model or heat partitioning model, implemented in the solver ANSYS-FLUENT version 14.5.0, the overall heat flux from the heated wall to the two-phase flow includes convective, quenching and evaporation heat flux. Furthermore, the heat flux partitioning model associates each of the heat flux contributions with a dimensionless wall area ratio, so as to define the ratio between heat flux contributions [1]. An important aspect is the knowledge and understanding of the fluid behavior in process of heat transfer. The thermophysical properties of water and steam are indicated as the fundamental properties that govern the process [3].

There are several ways to focus on the thermodynamic and transport properties: through different state equations and by a number of approximation functions. In the early 1990s, the appearance of safety analysis codes of nuclear facilities boosted the search on accuracy and expanded the range of water and steam properties. Then, the IAPWS new standards leveraged data and technological advances towards new formulations of thermodynamic properties [4].

* Supported by Algerian Atomic Energy Commission
† Corresponding author, mohammedi_brahim@hotmail.com

Artificial neural networks are being extensively used for predicting the 10 thermodynamic and transport properties mentioned above. Artificial neural network (ANN) is an advanced mathematical tool which determines the network output based on available experimental information. It also implies the mathematical function approximation for any linear and nonlinear systems [3, 5].

Gibbs phase rule allows one to determine the number of degrees of freedom or variance of a system. This is useful for interpreting phase diagrams.

$$F = 2 + C - p, \tag{1}$$

where F is the number of degrees of freedom, C is the number of chemical components and p is the number of phases in the system. The number two is specified because this formulation assumes that both p and T can be varied [6]. According to Eq. (1) in the two-phase region, corresponding to the saturation curve in the $(p-T)$ diagram, the thermodynamic properties of water and steam depend on a single state variable, temperature in our case. The range of prediction is valid along the entire vapor-liquid saturation line from 273.15 K to the critical temperature T_c, i.e., $273.150\,\mathrm{K} \leq T \leq 647.096\,\mathrm{K}$ [4].

The training of neural network is carried out by presenting a series of input data and target output values using experimental database including the entire range of validity where temperature is the single input parameter [4, 7–11].

II. ARTIFICIAL NEURAL NETWORKS APPROACH

Neural networks operate as a black box model requiring no detailed information about the system. It is an advanced mathematical modeling procedure inspired by biological neuron systems. The ANN approach seems to be completely suitable to the problems where the relations between variables are not linear and complex. In a multi-layer structure (Fig. 1), the neurons are grouped into layers, a layer of input neurons, a layer of output neurons and one or more hidden layers which are made up of many interconnected neurons.

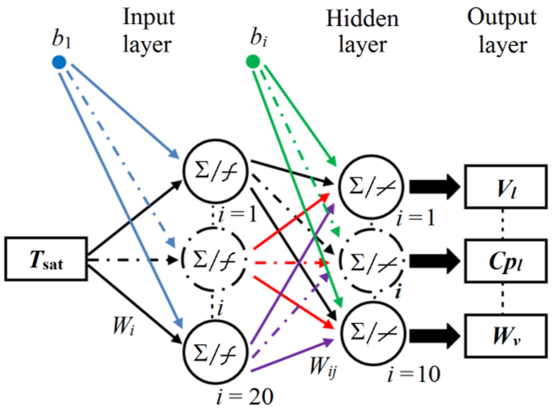

Fig. 1. (Color online) Structure of the ANN.

The normalization of values is a crucial step in the ANNs. The input values to the ANN may differ by several orders of magnitude, which may not reflect the relative importance of the inputs determining outlet thermophysical and transport properties. To this aim, the input data are normalized within the range of $[-1, 1]$ using a mapminmax algorithm, given by Eq. (2), to normalize the maximum and minimum values of each row. Against the output variables are normalized by log function [12].

$$y = \frac{(y_{\max} - y_{\min})(x - x_{\min})}{x_{\max} - x_{\min}} + y_{\min}. \tag{2}$$

After examining a considerable number of differently structured neural networks, the adequate ANNs selected in this paper have a single hidden layer with 20 neurons and an output layer with 10 neurons. The hidden layer has a tansig transfer function. The output layer has a purelin transfer function. Typical structure of the ANN is shown in Fig. 1. Single input variable (T: temperature) is the input, whereas 10 thermodynamic and transport properties of the density, specific heat, dynamic viscosity, thermal conductivity, and speed of sound, on saturated liquid and saturated vapor, are considered as the output variables.

Each neuron sums the product of each connection weight (w_{jk}) from a neuron (j) to the neuron (k) and input ($\mathbf{x}_j$), and the additional weight called the bias to get the value of sum for the neuron. The i^{th} neuron has a summer that gathers its weighted input $w_{ij} \cdot \mathbf{x}_j$ and the bias b_i to form its net input P_i [3].

$$P_i = \sum_{j=1}^{n-1} w_{ij}\mathbf{x}_j - b_i, \tag{3}$$

where w_{ij} denotes the strength of connection from the j^{th} input to the i^{th} neuron, $\mathbf{x}_j$ is the input vector; b_i is the i^{th} neuron bias. An activation function $F(P_i)$, the sigmoid function, is used to calculate the neuron output given the set of neuron inputs. To find suitable w_s and biases for each neuron, a process training is essential; it is the first step to build an ANN. Training means that the weights are corrected to produce prespecified ("correct", known from experiments) target values, and the training requires sets of pairs ($\mathbf{X}_S$, $\mathbf{Y}_S$) for input: the actual input into the network is a vector ($\mathbf{X}_S$), and the corresponding target is labeled ($\mathbf{Y}_S$) after successful training. When correct values of $\mathbf{Y}_S$ for each vector of $\mathbf{X}_S$ from the training set are obtained, it is hoped that the network will give correct predictions of Y for any new object of X according to the ANN model fundamentals and with the use of more data for training the network, better result would be obtained. The most utilized training method for multilayered neural network is called back propagation, where Levenberg-Marquardt (LM) is applied which is considered the most efficient algorithm in terms of speed and memory usage [13].

The number of observed data used in the ANN is 377 which are divided into three sections: the training set (275 data), test set (53 data) and validation set (49 data). Training, test and validation subsets of the ANN are obtained as selecting 72% of the dataset as training, 14% of the dataset as test and 14% of the dataset as validation subsets.

The differences between observed and predicted values are filtered back through the system and is used to adjust the connections between the layers, thus performance improves. The coefficient of root mean square error (*RMSE*) is the main criterion to evaluate the performance of ANN, which is defined as follows [3, 5]:

$$RMSE = \left[\frac{1}{n}\sum_{i=1}^{n}\left(\mathbf{y}_i - \mathbf{y}_i^t\right)^2\right]^{1/2}. \tag{4}$$

Statistical quality of the ANN for the training, test and validation sets is evaluated using the squared correlation coefficient R, absolute error AE and average absolute error AAE,

$$R = 1 - \frac{\sum_{i=1}^{n}\left(\mathbf{y}_i - \mathbf{y}_i^t\right)^2}{\sum_{i=1}^{2}\left(\mathbf{y}_i - \mathbf{y}_0\right)^2} \tag{5}$$

with

$$\mathbf{y}_0 = \frac{1}{n}\sum_{i=1}^{n}\left(\mathbf{y}_i - \mathbf{y}_i^t\right), \tag{6}$$

$$AE_i = \left[\frac{|\mathbf{y}_i^t| - |\mathbf{y}_i|}{|\mathbf{y}_i^t|}\right] \times 100, \tag{7}$$

$$AAE = \frac{1}{n}\sum_{i=1}^{n} AE_i, \tag{8}$$

where $\mathbf{y}_i$ represents either the i^{th} trained, test or validation output value and $\mathbf{y}_i^t$ is the corresponding target value, with n being the number of input vectors. The results are summarized in Table 1.

Observed and predicted (dynamic viscosity on saturated vapor as example) breakthrough curves shown in Fig. 2 indicate that the ANN describes the experimental data well.

Seen to the modeling performances, the general model obtained from the ANN belonging to all of the properties of water and steam was implemented in UDF that compiled and hooked in the solver ANSYS-FLUENT. Figure 3 shows the incorporation of UDF into the solver of a group of 8 properties (density, dynamic viscosity, thermal conductivity and speed of sound on saturated liquid and saturated vapor) and a group of 2 properties (specific heat on saturated liquid and saturated vapor). The UDF written in C++ is a routine which can be dynamically linked with the solver FLUENT and programmed by the user.

III. CFD CALCULATIONS WITH DEVELOPED UDF

A. Benchmark case

The proposed benchmark exercise, experimentally studied by Bartolemei and Chanturiya [14], is upward flow of subcooled water through a heated vertical tube of $\Phi 15.4\,\text{m} \times 2\,\text{m}$.

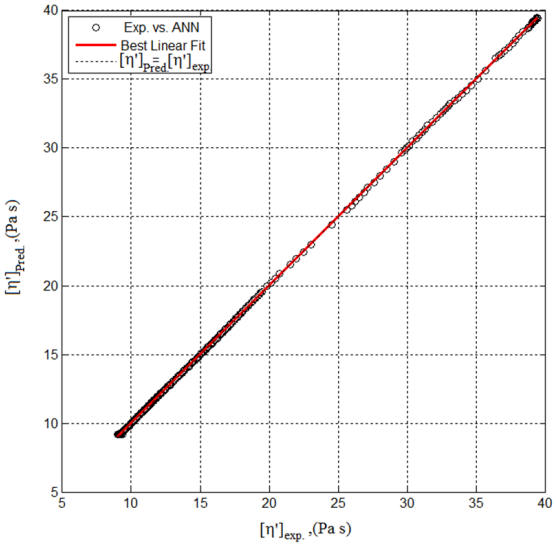

Fig. 2. (Color online) Comparison of target and ANN predicted values for dynamic viscosity on saturated vapor.

As shown in Fig. 4, the operating pressure is 4.5 MPa. The subcooled water, with the subcooling of 58.2 K, enters from the bottom side and travels upwards through the tube. The heat flux applied uniformly on the tube surface is $0.57\,\text{MW/m}^2$. The inlet mass flux is $900\,\text{kg/(m}^2\,\text{s)}$. The available experimental data include temperatures along the tube wall and axis, the bulk liquid temperature, and the cross-sectional averaged vapor volume fraction along the tube. The wall boiling is in the nucleate boiling regime [15, 16].

Parametric study is performed to investigate the effect of the developed UDF as summarized in Table 2.

B. Wall boiling model

In the nucleate subcooled boiling in a heated tube, the wall heat is partially used to form bubbles and the remaining portion is transferred to the liquid. The heat transfer from the wall in the vicinity of a nucleation site occurs during two distinct periods: the bubble growth time and the waiting time. According to the RPI, the total heat flux from a wall to liquid is partitioned into three parts [2, 17]

$$\dot{q}_{\text{wall}} = \dot{q}_{\text{C}} + \dot{q}_{\text{Q}} + \dot{q}_{\text{E}}, \tag{9}$$

where $\dot{q}_{\text{C}}$ is the single-phase convective heat flux, $\dot{q}_Q$ is quenching heat flux transferred to the liquid phase during the waiting time, and $\dot{q}_{\text{E}}$ is the heat flux associated with phase change, i.e., evaporation.

$$\dot{q}_{\text{C}} = h_c(T_{\text{w}} - T_{\text{l}})(1 - A_b), \tag{10}$$

where h_{c} is the liquid phase heat transfer coefficient; T_{w} and T_{l} are the wall and liquid temperature near the wall, respectively; and A_{b} is the portion covered by nucleation bubble.

$$\dot{q}_Q = \frac{2k_l}{\sqrt{\pi\lambda_l T}}(T_{\text{w}} - T_{\text{l}})A_{\text{b}}, \tag{11}$$

TABLE 1. Statistical performance of the trained ANN

Thermodynamic and transport properties	Best linear fit	R	RMSE	$AE_{\max}$ (%)	AAE (%)
Density(liquid)	$\boldsymbol{Y} = \boldsymbol{X} - 0.03100$	1	0.1936	0.2395	0.0681
Density(vapor)	$\boldsymbol{Y} = \boldsymbol{X} - 1.20000$	1	0.3143	0.6419	0.1518
Specific heat(liquid)	$\boldsymbol{Y} = \boldsymbol{X} + 0.02500$	1	0.3906	3.2169	0.3598
Specific heat(vapor)	$\boldsymbol{Y} = \boldsymbol{X} + 0.01600$	1	0.2513	2.4516	0.53
Dynamic viscosity(liquid)	$\boldsymbol{Y} = \boldsymbol{X} - 0.00800$	1	0.0881	1.0165	0.2498
Dynamic viscosity(vapor)	$\boldsymbol{Y} = \boldsymbol{X} - 0.00018$	1	0.0019	2.0948	0.1941
Thermal conductivity(liquid)	$\boldsymbol{Y} = \boldsymbol{X} + 0.39000$	1	0.0592	1.2867	0.2124
Thermal conductivity(vapor)	$\boldsymbol{Y} = \boldsymbol{X} + 0.00150$	1	0.0505	0.6982	0.2713
Speed of sound(liquid)	$\boldsymbol{Y} = \boldsymbol{X} - 0.00970$	1	0.0192	0.8621	0.1042
Speed of sound(vapor)	$\boldsymbol{Y} = \boldsymbol{X} - 0.00370$	1	0.0071	0.1805	0.0328

TABLE 2. Base case values

Parameters[a]	Value
Length (m)	2
Radius (mm)	7.7
Operating pressure (MPa)	4.5
Inlet mass flux (kg/(s m^2))	900
Heat flux (MW/m^2)	0.57
Inlet temperature (K)	473.15
Inlet subcooling (K)	58.2

[a] Wall, stainless-steel; fluid, H_2O

where k_l and λ_l are heat conductivity and diffusivity in the liquid phase and T is the period of bubble detachment.

$$\dot{q}_E = V_d N_w \rho_v h_{fv} f, \tag{12}$$

where V_d is the volume of the bubble based on the bubble departure diameter, N_w is the active nucleate site density, ρ_v is the vapor density, h_{fv} is the latent heat of evaporation, and f is the frequency of bubble departure.

Equations (9)–(12) require closure parameters with empirical relationship as frequency of bubble departure, bubble departure diameter, nucleate site density, etc.

C. UDF-RPI model validation

As the problem formulation is axisymmetric, the domain simulated is only a 2D slice with width equal to the tube radius. The code manual recommends using a quadrilateral computational mesh for Eulerian multiphase model, after several attempts to find the best computational meshes, we adopted grid with 80 uniform radial elements and 1000 uniform axial elements. Finer mesh density in a contact region (near the heated wall) to provide a better distribution of local flow parameters and to achieve a stable solution.

To ensure a fully-developed profile of velocity magnitude and turbulence quantities at the inlet, the outlet profiles of these quantities generated for a simulated flow field without boiling (single phase) will be used as inlet information to the boiling (multiphase) simulation.

The Eulerian-RPI method, which allows in FLUENT the modeling of multiple separate, yet interacting phases, is employed to predict the distribution of the local flow parameters, i.e., the vapor volume fraction, the bubble diameter and liquid temperature. The turbulence phenomena are described by a classical Re Normalisation Group (RNG) k-ε model in combination with enhanced wall treatment for the near-wall treatment. Value of $\mathbf{y}^+ = 5$ is considered reasonable for the enhanced wall treatment approach selected. See Table 3 for a more detailed list of input parameters and Table 4 for correlation of the boiling model used in benchmark case [18].

TABLE 3. Input parameters of subcooled nucleate boiling model

	Input	Value
Solver	Time	Steady
	Type	Pressure based
	Velocity formulation	Absolute
	2D space	Axisymmetric
Models	Energy	Active
	Viscous	RNG k-ε
	Near wall treatment	Enhanced
	Multiphase	Eulerian
	Drag	Ishii
	Lift	Moraga
	Turbulent dispersion	Lopez-De-Bertodano
	Turbulence interaction	Toshko-Hassan
	Heat transfer	Ranz-Marshall
	Interfacial area	Ia-Symmetric
	Bubble diameter	Sauter-Mean
	Mass transfer	RPI boiling

The saturation temperature at selected pressure is 530.55 K, the subcooled flow boiling model water properties are assumed to vary with temperature. It is technically part of the UDF we developed. That is the aim of this work.

The governing equations are non linear and several iterations of loop must be performed before a convergent solution is obtained. For the numerical accuracy, the first order upwind scheme is used for spatial discretization of set of governing equations. As the numerical scheme employed is coupled with volume fractions, a low courant number of 10 can be used to achieve faster convergence.

IV. RESULTS AND DISCUSSION

To validate the proposed UDF in conjunction with RPI wall boiling model, comparisons were made among the

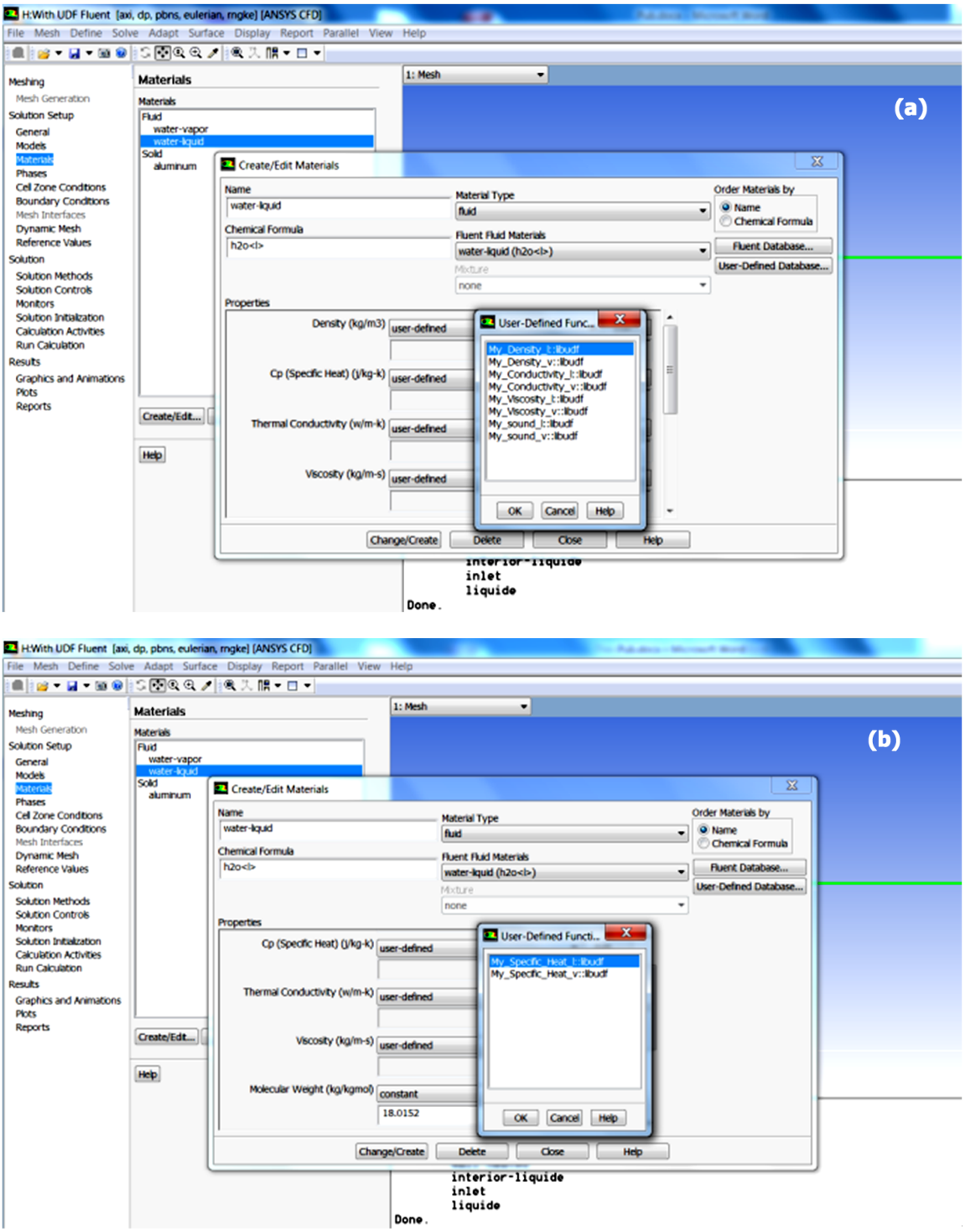

Fig. 3. (Color online) Developed UDF into CFD solver ANSYS-FLUENT. (a) Group of 8 properties; (b) Group of 2 properties.

RPI model, the RPI+UDF model, and experimental data of Bartolomei and Chanturiya for a heated vertical tube at 4.5 MPa [14]. The two models were with defining solution-dependent material properties as piecewise-linear functions of temperature using two data points at 473.15 K and 543.15 K. Figure 5(a) shows that the proposed UDF-RPI axial vapor volume fraction distribution agrees well with experimental data [14]. Idem for the liquid temperature profile along the tube. Figure 5(b) shows that the proposed UDF-RPI is in good agreement with the experimentally measured axial liquid temperature distributions. A comparison of the predictions with experimental data is demonstrated.

TABLE 4. Input parameters of subcooled nucleate boiling model

Bubble departure diameter	Frequency of bubble departure	Nucleation site density	Area influence coefficient
Tolubinski-Kostanchuk	Cole	Lemmert-Chawla	Delvalle-kennink

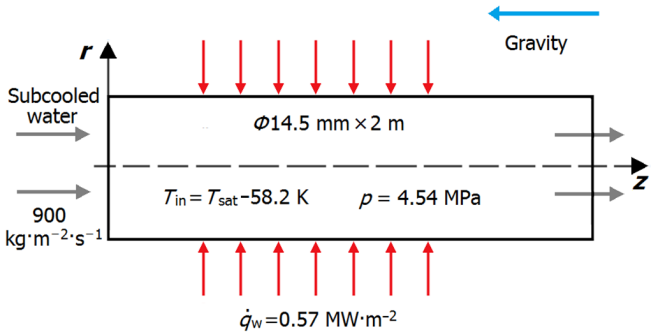

Fig. 4. (Color online) Geometry and flow conditions.

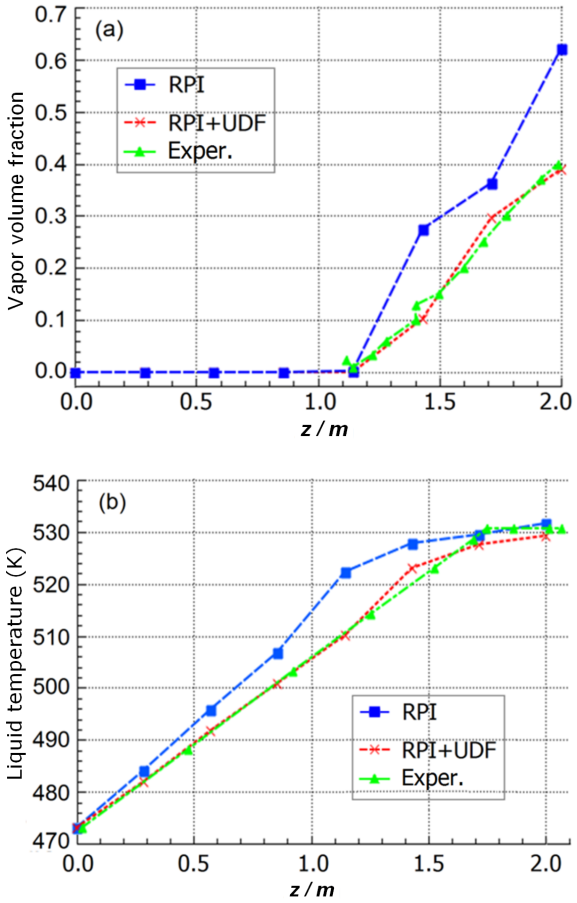

Fig. 5. (Color online) Comparisons of axial vapor volume fraction profile (a) and axial liquid temperature (b).

Parallel to works devoted to axial profiles of vapor volume fraction and liquid temperature, the radial distribution at various axial locations along the tube was evaluated. Figure 6 shows the radial profiles of vapor volume fraction and

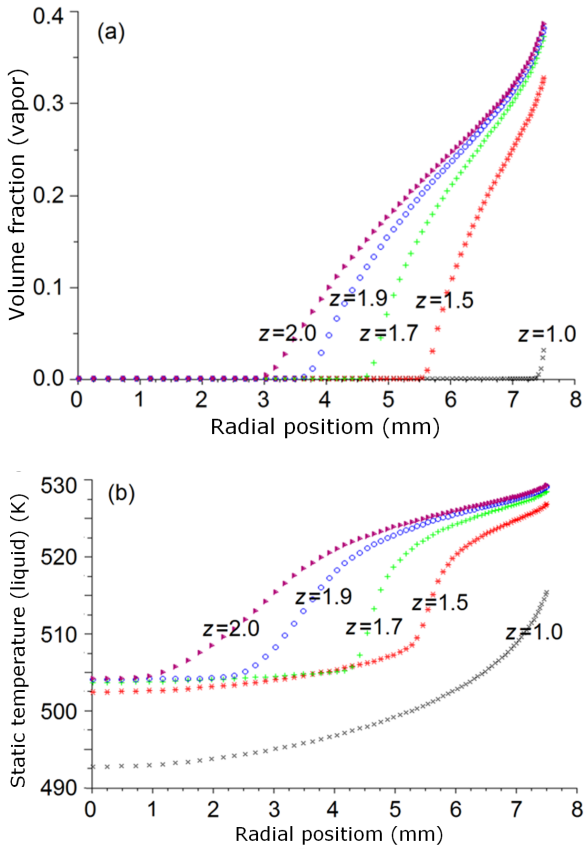

Fig. 6. (Color online) Profiles of vapor volume fraction (a) and liquid temperature (b) at 5 locations along the tube.

liquid temperature at 5 locations along the tube, for the proposed UDF in conjunction with RPI wall boiling model [19]. In Fig. 6(a), boiling is concentrated near the heated wall for the flow regime considered here. It is seen that the vapor volume fraction is substantially higher adjacent to the wall and decreases towards the center. Radial temperature profiles at 5 locations are shown in Fig. 6(b). The thermal non-equilibrium is evident. There are large temperature differences between the center and wall of the pipe at $z = 1.1$ m, where bubble production starts close to wall while the center temperature is below the saturation temperature. Non-equilibrium conditions decrease along the pipe and a radially uniform temperature distribution is reached around $z = 1.7$ m.

As a consequence of the comparison of the present study, it is clear that the case of UDF in conjunction with RPI wall boiling model, based on artificial neural networks is reasonable. This demonstrates the strong non-linearity of the forms of the thermophysical properties of water and steam often requires polynomial interpolations for defining solution-

dependent material properties, what makes the difference between the two models as compared to the experimental data of Bartolomei and Chanturiya, as shown in Fig. 5.

V. CONCLUSION

This work is focused on the numerical study of nucleate subcooled boiling in a heated tube using RPI Wall boiling model implemented in the solver ANSYS-FLUENT version 14.5.0 in conjunction with the developed UDF based on artificial neural networks that calculate the thermodynamic and transport properties on saturated liquid and saturated vapor of the water assumed to vary with temperature. The validation of the results has been made with the experimental data performed with the baseline case conditions. The results demonstrate that the RPI Neural-UDF method is able to predict reasonably well the vapor volume fraction distributions and liquid temperature profile in the heated vertical tube. The computed profiles of the vapor volume fraction and liquid temperature are in good agreement with available experiments. We remind that the maximum absolute error predicted by the artificial neural networks is around 3%. The ANN model exhibited a great potential in prediction of water and steam properties with the highest R and lowest RMSE values.

The developed UDF gives a simple and fast method to calculate water and steam properties depending on the temperature, and the present model correctly represents the nucleate boiling under pressurized conditions.

ACKNOWLEDGMENTS

The authors are grateful for the financial support and wish to thank A. Bousbia Salah for his many useful comments and suggestions to the manuscript of this work.

[1] Egorov Y and Menter F. Experimental implementation of the RPI wall boiling model in CFX-5.6. Technical report ANSYS, ANSYS Germany GmbH, TR-04-10, 2004.
[2] Kurul N and Podowski M Z. On the modeling of multidimensional effects in boiling tubes. Proceedings of the 27th National Heat Transfer Conference, Minneapolis, Minn, USA, 1991.
[3] Bouzidi A, Hanini S, Souahi F, *et al*. Viscosity calculation at moderate pressure for nonpolar gases via neural network. J Appl Sci, 2007, **7**: 2550–2455. DOI: 10.3923/jas.2007.2450.2455
[4] Wagner W and Kretzschmar H J. International steam tables, Second edition. Springer-Verlag Berlin Heidelberg, 2008.
[5] Ararem A, Bouzidi A, Mohamedi B, *et al*. Modeling of fixed-bed adsorption of Cs^{+} and Sr^{2+} onto clay-iron oxide composite using artificial neural network and constant-pattern wave approach. J Radioanal Nucl Chem, 2014, **301**: 881–887. DOI: 10.1007/s10967-014-3200-4
[6] Wagner W and Prub A. The IAPWS formulation 1995 for the thermodynamic properties of ordinary water substance for general and scientific use. J Phys Chem, 2002, **31**: 387–535. DOI: 10.1063/1.1461829
[7] Su G, Fukuda K, Morita K, *et al*. Application of artificial neural network for the prediction of flow boiling curves. J Nucl Sci Technol, 2002, **39**: 1190–1198. DOI: 10.3327/jnst.39.1190
[8] Washburn E W. International critical tables of numerical data, physics, chemistry and technology. knovel, Norwich, 2003.
[9] Chase M W, Davies C A, Downey J R, *et al*. JANAF thermochemical tables. J Phys Chem Ref Data, Suppl. 1, **14**, 1985.
[10] Yaws C L. Chemical properties handbook. McGRAW-HILL, 2006.
[11] Rogers G F C and Mayhew Y R. Thermodynamic and transport properties of fluids: SI units. Blackwell Publishing Ltd, 2004.
[12] Demuth H, Beale M and Hagan M. Matlab, neural network toolbox 6, User's Guide. MathWorks, Inc., 2009.
[13] Oguz E and Ersoy M. Removal of Cu^{2+} from aqueous solution by adsorption in a fixed bed column and Neural Network Modelling. Chem Eng J, 2010, **164**: 56–62. DOI: 10.1016/j.cej.2010.08.016
[14] Bartolomei G G and Chanturiya V M. Experimental study of true void fraction when boiling subcooled water in vertical tubes. Therm Eng+, 1963, **14**: 123–128.
[15] Bartolomei G G and Gorburov V I. Experimental study of vapour phase condensation in liquid subcooled below saturation temperature. Heat Prod, 1969, **12**: 58–62.
[16] Li H, Punekar H, Vasquez S A, *et al*. Prediction of boiling and critical heat flux using an Eulerian multiphase boiling model. IMECE, Colorado, USA, 2011.
[17] Regab R and Wang T. Investigation of applicability of using water mist for cooling high-pressure turbine components via rotor cavity feed tubes. Proceedings of HT2013, ASME summer heat transfer conference, Minneapolis, MN, USA, 2013.
[18] Wilcox M P. Mathematical modeling of convective heat transfer: single phase through subcooled boiling flows. Rensselaer Polytechnic Institute Hartford, Connecticut, 2013.
[19] Mat M D, Aldas K and Kaplan Y. Numerical investigation of subcooled boiling in a vertical pipe using a bubble-induced turbulence model. Turkish J Eng Env Sci, 2002, **26**: 275–284.